

Size versus electronic factors in transition metal Laves phase stability

This article has been downloaded from IOPscience. Please scroll down to see the full text article.

1990 J. Phys.: Condens. Matter 2 8189

(<http://iopscience.iop.org/0953-8984/2/41/006>)

View [the table of contents for this issue](#), or go to the [journal homepage](#) for more

Download details:

IP Address: 171.66.16.151

The article was downloaded on 11/05/2010 at 06:55

Please note that [terms and conditions apply](#).

LETTER TO THE EDITOR

Size versus electronic factors in transition metal Laves phase stability

Yukinori Ohta† and D G Pettifor‡

† Department of Applied Physics, Nagoya University, Chikusa-ku, Nagoya 464-01, Japan

‡ Department of Mathematics, Imperial College of Science, Technology and Medicine, London SW7 2BZ, UK

Received 15 August 1990

Abstract. The different roles played by atomic size and electronic factors in stabilizing the transition metal Laves phases against the two competing phases $C11_b(\text{MoSi}_2)$ and $C16(\text{CuAl}_2)$ are studied within a simple tight binding d bond model. Good qualitative agreement with the experimental AB_2 structure map is found if size and electronic factors are both included.

The AB_2 Laves phases are the best known examples of size-factor compounds in which the relative sizes of the atoms are important in determining the structural stability. For the Laves phases the closest packing of the two types of constituent atoms occurs for the radius ratio $r_A/r_B = \sqrt{3}/\sqrt{2} = 1.225$ (see for example [1]). In practice, however, the ratio of the Goldschmidt atomic radii of the pure elements forming the phases varies from 1.05 to 1.68 [2]. Thus, other factors such as the average number of electrons per atom or e/a ratio must also be important [3–6]. In this letter we examine within a simple tight binding model the stability of the transition metal Laves phases relative to two other competing phases, namely the BCC-based $C11_b(\text{MoSi}_2)$ structure type and $C16(\text{CuAl}_2)$. We will see that the structural energy difference theorem [7] allows us to separate out the different roles played by atomic size differences and electronic factors.

Figure 1 shows the experimental structure map ($\mathcal{M}_A, \mathcal{M}_B$) for the AB_2 transition metal compounds. The phenomenological coordinate \mathcal{M} is the so-called Mendeleev number which orders all the elements in the periodic table with respect to one another [18]. We see that the $C14(\text{MgZn}_2)$, $C15(\text{MgCu}_2)$ and $C36(\text{MgNi}_2)$ Laves phases are all located above the diagonal $\mathcal{M}_A = \mathcal{M}_B$, whereas the $C16(\text{CuAl}_2)$ domain is located below it. Moreover, we see that the Laves phases reach down towards the diagonal in the vicinity where the BCC lattice is most stable for the elemental group VA and VIA transition metals. On the other hand, compounds with the $C11_b(\text{MoSi}_2)$ structure type, which is derived from the BCC lattice by stacking pure A or pure B {100} planes together, are found only at the upper left-hand and lower right-hand corners of the map, far away from the diagonal. We now show that this behaviour can be accounted for theoretically.

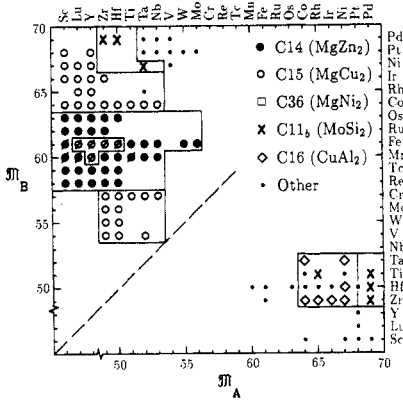


Figure 1. The structure map for the AB_2 transition metal compounds. The symbols with slashes indicate magnetic phases.

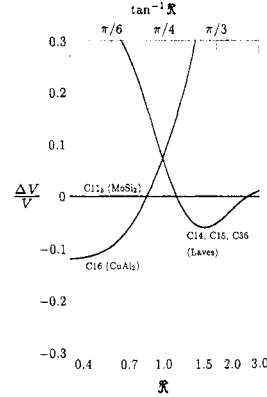


Figure 2. The fractional change in prepared volume $\Delta V/V$ with respect to the $C11_b(\text{MoSi}_2)$ lattice versus the relative size factor R .

The tight binding (TB) d bond model is the simplest scheme for describing the energetics of transition metal compounds within a quantum mechanical framework [9–11]. The total binding energy per AB_2 formula unit may be written in the form

$$U = U_{\text{rep}} + U_{\text{bond}} \quad (1)$$

where U_{rep} is a semiempirical pairwise repulsive contribution and U_{bond} is the covalent d bond energy which results from computing the local density of states $n_i(\epsilon)$ at site i within the two-centre, orthogonal tight binding approximation. That is,

$$U_{\text{bond}} = \mathcal{N}^{-1} \sum_i \int^{\epsilon_F} (\epsilon - \epsilon_i) n_i(\epsilon) d\epsilon \quad (2)$$

where ϵ_i is the atomic d energy level at site i , ϵ_F is the Fermi energy and \mathcal{N} is the number of AB_2 formula units in the crystal. The bond energy is evaluated under the constraint that each site is locally charge neutral, the A and B sites being characterized by N_A and N_B valence d electrons respectively. The simple form of equation (1) may be derived from first principles (see [12] and references therein). The pairwise nature of the repulsive term follows directly from the Harris–Foulkes approximation [13, 14] to density functional theory, whereas the Hückel-type two-centre orthogonal form of the matrix elements may be justified in principle within Anderson’s chemical pseudopotential theory [15, 16].

The bond energy was evaluated for the different structure types assuming canonical TB bond integrals $dd(\sigma, \pi, \delta) = (-6, 4, -1)h(R)$ where

$$h_{AA(BB)}(R) = (C_{A(B)})/R^5 \quad (3)$$

where R is the internuclear separation and C_A, C_B are constants characteristic of the A, B constituents [17]. The AB bond integrals are given by the geometric mean of the AA and BB hopping integrals. The repulsive pairwise interactions between the different sites were assumed to be proportional to the square of the hopping integrals $h(R)$, namely

$$\phi_{AA(BB)}(R) = k(C_{A(B)}/R)^{10} \quad (4)$$

where k is the constant of proportionality and ϕ_{AB} is given by the geometric mean. This

Table 1. The structure coefficients $\alpha_{it'}$. The number of atoms included in the summation of equation (6) is indicated in parentheses. The Pearson symbol gives the symmetry of the unit cell (cubic, hexagonal or tetragonal) and the number of atoms per unit cell.

Structure type	Pearson symbol	α_{AA}	α_{BB}	α_{AB}
C11 _b (MoSi ₂)	tI6	5.378(16)	57.241(74)	92.971(84)
C14 (MgZn ₂)	hP12	5.744(16)	129.351(58)	52.817(54)
C15 (MgCu ₂)	cF24	5.744(16)	129.303(60)	52.866(56)
C36 (MgNi ₂)	hP24	5.744(16)	129.327(59)	52.842(55)
C16 (CuAl ₂)	tI12	23.056(6)	34.205(22)	141.872(16)

simplifying assumption that $\phi(R)\alpha(h(R))^2$ is capable of reproducing the behaviour of the band width, cohesive energy, equilibrium volume and bulk modulus across the elemental 4d and 5d transition metal series (see figure 30 of [10]).

It follows that the repulsive energy per AB₂ formula unit may be written

$$U_{\text{rep}} = 1.5 k \Omega^{-10/3} C_A^5 C_B^5 (\alpha_{AB} + \mathcal{R}^5 \alpha_{AA} + \mathcal{R}^{-5} \alpha_{BB}) \quad (5)$$

where Ω is the volume per formula unit. The volume-independent but structure-dependent coefficients $\alpha_{it'}$ are defined by

$$\alpha_{it'} = (3N)^{-1} \sum (\Omega^{1/3}/R)^{10} \quad (6)$$

where the sum extends over the relevant AA, BB or AB interactions on the lattice and $3N$ gives the total number of atoms in the crystal. Table 1 gives the values of the coefficients $\alpha_{it'}$ for the five different structure types shown in figure 1, assuming $c/a = 0.8324$ and $u = 1/6$ for the C16(CuAl₂) lattice [18]. \mathcal{R} is the relative size factor which is defined by $\mathcal{R} = C_A/C_B$. It is a direct measure of the relative size of the A and B atoms since it follows from equation (4) that AA and BB atomic pairs experience the same repulsive energy for internuclear separations $R_{AA} = 2r_A$, $R_{BB} = 2r_B$ such that

$$r_A/r_B = C_A/C_B = \mathcal{R}. \quad (7)$$

The relative importance of size and electronic factors in determining the structural trends in figure 1 can be studied directly by using the structural energy difference theorem [17]. This theorem states that the energy difference between any two equilibrium structures of a system characterized by a binding energy law of type (1) is given to first order by

$$\Delta U = (\Delta U_{\text{bond}})_{\Delta U_{\text{rep}}=0}. \quad (8)$$

That is, the relative stability of two structures is determined solely by the bond energy provided their volumes have first been prepared so that the different lattices display the same repulsive energy.

This theorem is very important because it allows the relative stability of different structures to be interpreted within a two-step process which makes immediate contact with one's physical intuition [19]. In the first step the volumes of the different structure types are adjusted to guarantee the same repulsive energy. This stage depends only on the nature of the repulsive interaction and reflects the relative atomic sizes of the constituents through equation (7). It generalizes the usual classical procedure of packing

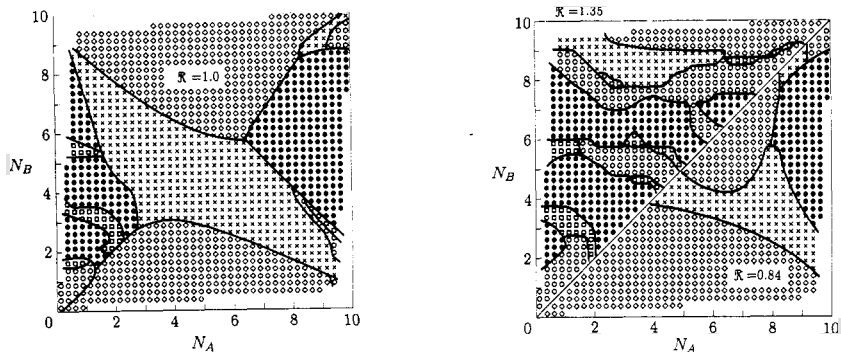


Figure 3. The theoretical structure maps (N_A, N_B) for $\mathcal{R} = 1$ (left-hand panel) and $\mathcal{R} = 1.35$ and 0.84 (right-hand panel).

together hard spheres until they touch. In the second step the bond energies are compared at these prepared volumes in order to see which structure is most stable. This corresponds in the ionic limit to the customary practice of comparing Madelung energies. In the present case of metallic compounds it reflects the electronic factor through the occupancy of the bands and bonding states.

The first step, therefore, is to prepare the volumes of the different structures so that they experience the same repulsive energy as some reference lattice which we have taken to be the BCC-based $C11_b(\text{MoSi}_2)$ structure type. It follows from (5) that the difference in volume ΔV is given to first order by

$$\frac{\Delta V}{V} = \frac{3}{10} \frac{\Delta\alpha_{AB} + \mathcal{R}^5 \Delta\alpha_{AA} + \mathcal{R}^{-5} \Delta\alpha_{BB}}{\alpha_{AB} + \mathcal{R}^5 \alpha_{AA} + \mathcal{R}^{-5} \alpha_{BB}} \quad (9)$$

where the $\Delta\alpha_{tt'}$ are the corresponding differences in the repulsive coefficients. Thus, the fractional change in volume is a function only of the relative size factor \mathcal{R} so that a universal curve may be plotted for each structure type (with a given set of internal coordinates) as shown in figure 2.

We see that for $\mathcal{R} = 1$ the BCC-based lattice $C11_b(\text{MoSi}_2)$ is more closely packed than either the Laves phases or $C16(\text{CuAl}_2)$. However, as expected, as \mathcal{R} increases the Laves phases assume a more compact lattice than BCC for $\mathcal{R} > 1.13$. In the limit as \mathcal{R} tends to infinity, the Laves phases again have a larger volume as the A atoms of the cubic $C15$ phase, for example, sit on a tetrahedrally coordinated diamond lattice [1] whereas those of the $C11_b$ phase sit on a six-fold coordinated simple cubic lattice. We see that the $C16(\text{CuAl}_2)$ structure type behaves in just the opposite manner, becoming more compact as \mathcal{R} decreases. Whereas the A atom in the AB_2 Laves phase is surrounded by a coordination polyhedron containing twelve B atoms and four A atoms, that in the $C16(\text{CuAl}_2)$ phase is surrounded by a coordination polyhedron containing only eight B atoms and two A atoms (see figure 3 of Villars *et al* [20] and figure 29.17 of Wells [11]).

The left-hand panel in figure 3 shows the predicted structure map for the case where the atoms have identical size. It was calculated by comparing the bond energies $U_{\text{bond}}(N_A, N_B)$ of the five different structure types at the prepared volumes corresponding to $\mathcal{R} = 1$ taking the $C11_b(\text{MoSi}_2)$ lattice with $a = 11.65$ au, $c = 9.70$ au as reference [18] and choosing $C_A = C_B = 2.29$ au corresponding to the group VIA

transition element molybdenum [17]. The energy bands and corresponding local densities of states were evaluated for nearly 50 different values of the atomic energy level mismatch $E_{AB} = E_A - E_B$ (ranging from -0.32 to $+0.32$ Ryd) using direct diagonalization of the TB Hamiltonian and sampled over up to 700 k -points in the irreducible Brillouin zone within the tetrahedron method [22]. For each choice of atomic energy level mismatch E_{AB} and average band filling \bar{N} we can compute the corresponding electron occupancies N_A and N_B on the A and B sites respectively so that for each structure type we have the bond energy U_{bond} with respect to a very fine mesh within the (N_A, N_B) plane.

The $\mathcal{R} = 1$ structure map in figure 3 shows that the BCC-based lattice $C11_b(\text{MoSi}_2)$ is the most stable for an average band filling centred about $\bar{N} = 4$. This is not unexpected in the vicinity of the diagonal $N_A = N_B$ since the BCC group VA and VIA transition elements are stable here. However, we see that as the size of the atomic energy level mismatch increases (corresponding to $|\Delta N|$ increasing), the $C11_b$ stability remains although the domain narrows. This causes the Laves domains in the upper half diagonal to be restricted to a relatively small region. Thus, the electronic contribution is not sufficient by itself to stabilize the Laves phases over the broad area which is observed experimentally in figure 1.

The right-hand panel in figure 3 shows the results of increasing the relative size factor to $\mathcal{R} = 1.35$ (in the upper half diagonal where $C_A > C_B$) or decreasing it to $\mathcal{R} = 0.84$ (in the lower half diagonal where $C_A < C_B$). As expected from the behaviour of the atomic volumes in figure 2, the increase in the size factor has now stabilized the Laves phases over a much larger area in agreement with experiment, whereas the decrease in the size factor has extended the stability of the $C16(\text{CuAl}_2)$ domains. We see that the right-hand panel of figure 3 is now in good qualitative agreement with the experimental structure map in figure 1. In the upper half diagonal the Laves phases are correctly ordered amongst themselves, changing from cubic (C15) to hexagonal (C14) back to cubic (C15) as the \mathcal{M}_B or N_B increases. (Note that the small C15 domain for $N_B = 60$ (Mn) and 61 (Fe) is due to the presence of magnetism [23].) In addition, the upper cubic Laves domain gives way to a small BCC-based $C11_b$ domain as found experimentally. In the lower half diagonal we predict the correct relative ordering of the observed $C16(\text{CuAl}_2)$ and $C11_b(\text{MoSi}_2)$ domains. The predicted Laves domains occur in a region of positive heat of formation and thus not found experimentally.

In conclusion, we have studied the different roles played by size and electronic factors in stabilizing the transition metal Laves phases against two competing phases, namely the BCC-based $C11_b(\text{MoSi}_2)$ structure type and $C16(\text{CuAl}_2)$. Good qualitative agreement with the experimental AB_2 structure map is found only if both size and electronic factors are taken into account within the simple TB model.

One of the authors (YO) gratefully acknowledges stimulating conversations with Professor J Hafner. The work was supported in part by a Grant-in-Aid for Encouragement of Young Scientists from the Japanese Ministry of Education, Science and Culture. The computations were carried out on the HITAC M-680H at the Computer Centre of the Institute for Molecular Science, Okazaki National Research Institute, and FACOM M-382 and M-780/20 at the Nagoya University Computer Centre.

References

- [1] Wells A F 1986 *Structural Inorganic Chemistry* (Oxford: Clarendon)

- [2] Dwight A E 1960 *Trans. Am. Soc. Metals* **53** 477
- [3] Hume-Rothery W, Smallman R E and Haworth C W 1969 *The Structure of Metals and Alloys* (London: Institute of Metals)
- [4] Phillips R B and Carlsson A E 1989 in *Atomistic Simulation of Materials: Beyond Repair Potentials* ed V Vitek and D J Srolovitz (New York: Plenum)
- [5] Turchi P and Ducastelle F 1985 in *The Recursion Method and its Applications* ed D G Pettifor and D L Weaire (Berlin: Springer) p 104
- [6] Johannes R L, Haydock R and Heine V 1976 *Phys. Rev. Lett.* **36** 372
- [7] Pettifor D G 1986 *J. Phys. C: Solid State Phys.* **19** 285
- [8] Pettifor D G 1988 *Mater. Sci. Technol.* **4** 675
- [9] Ducastelle F 1970 *J. Physique* **31** 1055
- [10] Pettifor D G 1987 *Solid State Phys.* **40** 43
- [11] Ohta Y, Finnis M W, Pettifor D G and Sutton A P 1987 *J. Phys. F: Met. Phys.* **17** L273
- [12] Sutton A P, Finnis M W, Pettifor D G and Ohta Y 1988 *J. Phys. C: Solid State Phys.* **21** 35
- [13] Harris J 1985 *Phys. Rev. B* **31** 1770
- [14] Foulkes W M C and Haydock R 1989 *Phys. Rev. B* **39** 12520
- [15] Anderson P W 1968 *Phys. Rev. Lett.* **21** 13
- [16] Skinner A J and Pettifor D G 1990 to be published
- [17] Pettifor D G 1977 *J. Phys. F: Met. Phys.* **7** 613
Anderson O K, Klose W and Nohl M 1978 *Phys. Rev. B* **17** 1209
- [18] Wyckoff R W G 1963 *Crystal Structures* (New York: Wiley)
- [19] Pettifor D G and Podloucky R 1986 *J. Phys. C: Solid State Phys.* **19** 315
- [20] Villars P, Mathis K and Hulliger F 1989 in *The Structures of Binary Compounds, Cohesion and Structure* vol 2, ed F R de Boer and D G Pettifor (Amsterdam: North Holland) p 1
- [21] Cyrot-Lackmann F 1968 *J. Phys. Chem. Solids* **29** 1235
- [22] Rath J and Freeman A J 1975 *Phys. Rev. B* **11** 2109
- [23] Ohta Y, Miyauchi M and Shimizu M 1989 *J. Phys.: Condens. Matter* **1** 2637
Asano S private communication